Environmentally Induced Failure of Gold Jewelry Alloys

Colin C. Merriman, David F. Bahr, and M. Grant Norton
School of Mechanical and Materials Engineering, Washington State University, Pullman, WA 99164-2920
E-mail: norton@mme.wsu.edu

Abstract

Stress corrosion cracking (SCC) is an established form of environmental attack in low karatage gold jewelry alloys. The cause of failure is often attributed to exposure to chlorinated solutions. At a certain gold content (usually greater than 14K) the alloy is widely believed protected from SCC. In this study, three commercial 18K gold alloys (yellow gold, nickel white gold, and palladium white gold) were tested in combination with three different household solutions to determine relative corrosion rates. These rates were determined using polarization tests. Once the maximum corrosion rate had been established, SCC tests using the constant potential dead weight method were used to determine time to failure. The resultant failure surfaces were examined to determine mode of fracture, which in all cases was predominantly intergranular. It was found that corrosion rates depended upon both the alloy system and the test solution. SCC was clearly demonstrated in 18K gold alloys, although in all cases times to failure were significantly greater than has been reported for lower karatage alloys. Palladium white gold was far more resistant to SCC than the other systems studied.

Introduction

From a hoard discovered in an ancient burial ground at Varna, Bulgaria we know that the use of gold dates back to at least 4600-4200 BCE. Since its first discovery gold has been used in jewelry not only because of its beauty and resistance to corrosion, but also because it is easier to work than all other metals. The manufacture of gold jewelry uses about 2000 tons of gold per annum making it the most important single component of the entire gold market (1).

Because of its extreme ductility and softness there are several drawbacks in the use of pure gold (24 karat) for jewelry applications. However, pure gold (locally known as 'Chuk Kam') jewelry is dominant in the Chinese region of Asia (2). In other parts of the world, it is more common to find gold alloyed with other metals including copper, nickel, palladium, and silver to increase its strength and hardness. The addition of these elements also imparts distinctive colors to the alloy. Yellow gold contains a mixture of copper, silver, and zinc. There are two types of white gold in common use. The nickel white golds usually contain nickel with copper and zinc as alloying additions. The palladium white golds are alloys of palladium, silver and often some copper and zinc. These alloys can also vary in gold content: 10 karat – 41.7 wt.% Au; 14 karat – 58.5 wt.% Au; 18 karat – 75 wt.% Au, and 22 karat – 91.6 wt.% Au.

For many years 14 karat (14K) yellow and white gold have been the dominant commercial alloys for jewelry applications in the United States, but more recently there has been an increased demand for 18K gold. Despite their higher gold content these alloys appear to be susceptible to in-service failure, which is often attributed to chlorine corrosion. Figure 1 shows an image of an 18K nickel white gold die struck setting that failed in use. Failure is typically characterized by a "rock candy" intergranular fracture surface, Figures 2a and 2b, that can be attributed to stress corrosion cracking (SCC). Similar failures can also occur with investment cast settings

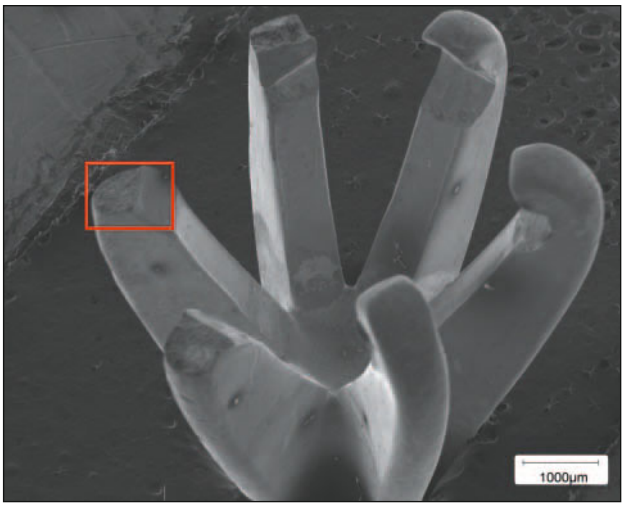

Figure 1
SEM image of an 18K nickel white gold setting that failed after 3 years in service

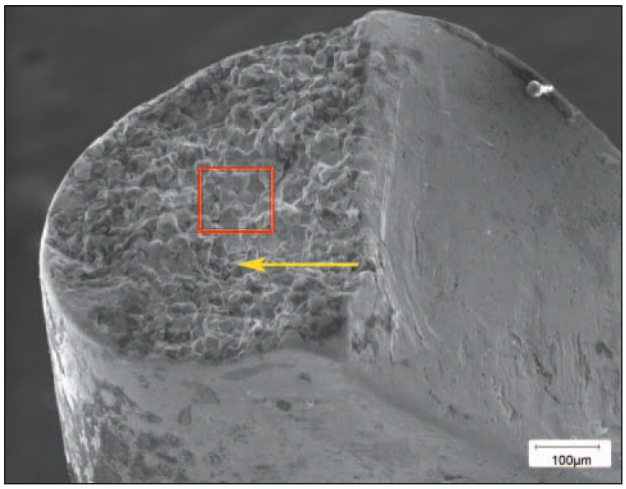

Figure 2(a)
Magnified view of fractured prong on 18K nickel white gold setting. Arrow indicates the direction of probable crack propagation

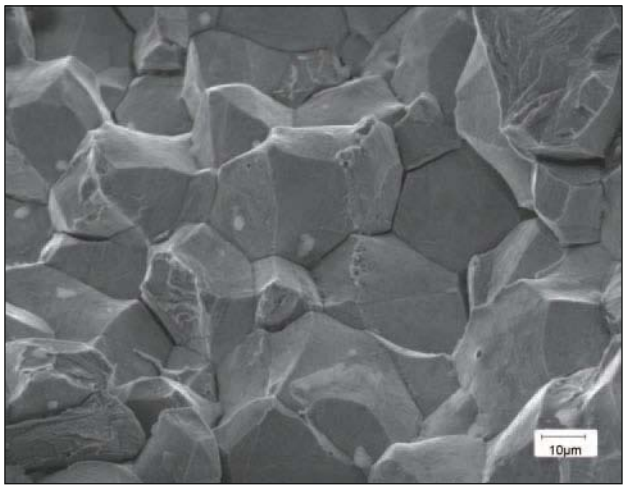

Figure 2(b)
SEM image showing primarily intergranular SCC in 18K nickel white gold

and it is this method of manufacture that was used to produce the material used in this present study.

SCC of Cu-Au alloys containing 50 at.% or less of gold has been studied extensively and various failure modes and mechanisms proposed (see, for example, Refs. 3-8). The lower karatage jewelry alloys are well known to be susceptible to SCC (9). Alloys with higher gold concentrations are often assumed protected from stress corrosion. Corrosion of 18K yellow gold has been reported to occur in certain environments, specifically in aqueous chloride solutions containing the Au^{3+} ion at the Au/Au^{3+} equilibrium potential (10). Chlorine has been the subject of scrutiny for the corrosion of gold alloys because of its inherently corrosive nature and abundance in many commercial cleaning products and other common fluids.

Intergranular SCC (IGSCC) is an anodic process with an initial induction period where the crack nucleates at a microscopic level on a grain boundary. The crack propagates intergranularly due to the high grain boundary energy until a critical velocity and stress intensity is achieved for fracture to continue transgranularly. The higher energy region can be attributed to thin layers along the boundaries being depleted in certain alloying elements that have the highest oxidation potential, creating a high stress region. This process is referred to as de-alloying and shows sharp 'parting limits', which refer to the critical concentration of the more active component above which it can be removed electrochemically from the alloy in an appropriate oxidizing environment. Thus the parting limit is related to the Tammann effect observed for superficial corrosion (11).

Yellow gold has been found to have the highest failure rate in service followed by nickel white gold. Nickel white gold is also susceptible to "fire cracking", which can occur during rapid cooling following annealing and is due to residual internal stresses. Failure in palladium white gold has never been reported. It should be noted that palladium white gold is rarely used in the United States as a setting due primarily to its expense and to difficulties in investment casting of the alloy. This present study focuses on SCC of three commercially available18K gold jewelry alloys in a series of common solutions.

Table 1
Composition of Gold Alloys Studied (wt.%)

Alloy	Au	Cu	Ag	Ni	Zn	Pd	HV*
18K yellow gold	75.2	13.9	9.0	-	1.9	-	125
18K Ni white gold	75.2	12.8	-	8.5	3.5	-	265
18K Pd white gold	75.0	6.0	-	-	4.0	15	130

* Vickers hardness

1 Experimental Method

The alloys used were prepared from 0.08 cm diameter wire of three different compositions shown in Table 1. Both the yellow gold and nickel white gold alloys were obtained from Hoover and Strong. The palladium white gold was obtained from Imperial Ready Stock. Each wire was melted down and cast in a standard gypsum-bonded investment using a broken-arm centrifugal investment casting process, where the molten metal is spun into the investment plaster cast. The casts were then removed from the jig and placed on a ceramic tile and allowed to air cool for between 30 and 45 minutes. The melting and casting was performed to simulate the microstructures of the cast jewelry settings. After casting the samples were removed from the investment plaster, washed in acetone, methanol, and toluene as part of the standard processing by which jewelry casting is performed, and dried in a convection oven at 150°C for 15 minutes. The wires were measured with a micrometer to ensure a final cast length of 11 cm with a diameter of 0.08 cm.

The corrosive solutions investigated were commercially available bleach, swimming pool water, and hot tub water each with varying amounts of chlorine, as shown in Table 2. The latter two solutions were prepared by a certified hot tub and

Table 2
Solutions Studied for Electrochemical Polarization

Solution/Active ingredient	Application	pH	Free Cl^- (ppm)	Total Cl (ppm)
1. Hydrochloric acid (HCl)	Swimming pool	7.3	2.2	2.8
2. LiquiChlor (16% NaHClO) Caustic soda (NaOH)	Hot tub	7.2	3.0	4.0
3. Bleach# (3% NaHClO)	General cleaner	11.5	4860	37900

Clorox

swimming pool contractor and tested to ensure the solutions were consistent with that of in-service locations. The electrode potentials were measured through an EG&G PARC 173 potentiostat-galvanostat with an Ag/AgCl reference electrode and graphite counter electrode. The potentials are reported versus the silver/silver chloride (Ag/AgCl) electrode. All experiments were carried out at room temperature.

Anodic polarization experiments were performed to determine the maximum "corrosion rate" of each alloy in solution. While strictly not a corrosion rate (a term usually reported in loss of material per time under a given environmental condition), the anodic current density measured in these studies can be related to material loss by

$$C = K\frac{ai}{nD} \quad (1)$$

where C is the corrosion rate in μm/year, a is the atomic weight of the dissolved species, i is the measured current density in μA/cm², n is the valence charge of the dissolved species, and D is the density of the material. K is a constant, 3.27 for conversion to μm/year (12). However, because the samples tested are alloys, which may undergo preferential dissolution of one alloy component, we report all "corrosion rates" in this paper as current densities, which will scale directly with actual corrosion rates. A conventional three electrode glass Green cell was used for the measurements (13). The solution was introduced into the cell with the sample and allowed to reach a steady state potential for 15 minutes. Polarization began at a voltage 10% below the open circuit potential. A scanning rate of 1 mVs^{-1} was used. After each polarization test was completed, the sample was removed and a solution of 3% NaHS in de-ionized water was titrated into the polarization solution to detect the presence of $CuCl_2$, $NiCl_2$, or $PdCl_2$ via the precipitation of CuS, NiS, or PdS, respectively. The final precipitate was removed and allowed to dry and its chemical constituents determined by energy dispersive spectrometry (EDS). This analysis would indicate a selective dissolution of the less noble element in each alloy resulting in a Cu, Ni, or Pd depleted area along the grain boundaries.

Once a maximum corrosion rate was determined for each alloy system in a given solution, dead-weight-loading tests were performed to determine time to failure under a constant load of 20 kg. This load corresponds to a stress of 195 MPa for these wires, which is between 10-20% below the yield point for all three alloys. A 0.01 cm deep "crack" was cut into the wire with a 1 mm thick diamond wafer blade. A conventional three electrode glass cell was once again used, this time with a hole in the bottom of the cell for the wire to pass through and connect to the 20 kg weight. The solution was added and the system allowed to reach an open circuit potential for 15 minutes. The sample was anodically polarized to an appropriate potential to attain the maximum corrosion rate determined from the previous polarization experiments. Time to failure was measured from this point. After failure, the exposed surfaces were examined with a JEOL JSM-6400 scanning electron microscope (SEM) to determine the mode of fracture and chemical variations on the fracture surface.

2 Results

Polarization Curves

Figure 3 shows polarization curves for the yellow gold alloy in the three solutions. Note that only the anodic polarization regions are shown for clarity. The open circuit corrosion potential for the alloy in hydrochloric acid solution and caustic soda-LiquiChlor are at -0.12 V and -0.13 V, respectively. In bleach the corrosion potential of the same alloy is 0.55 V. In the caustic soda and hydrochloric acid solutions, there is a distinct active corrosion region prior to passivation at approximately 0.2 V. The sample tested in the bleach solution does not undergo this active-passive transition. For all three solutions above the corrosion potential the current density

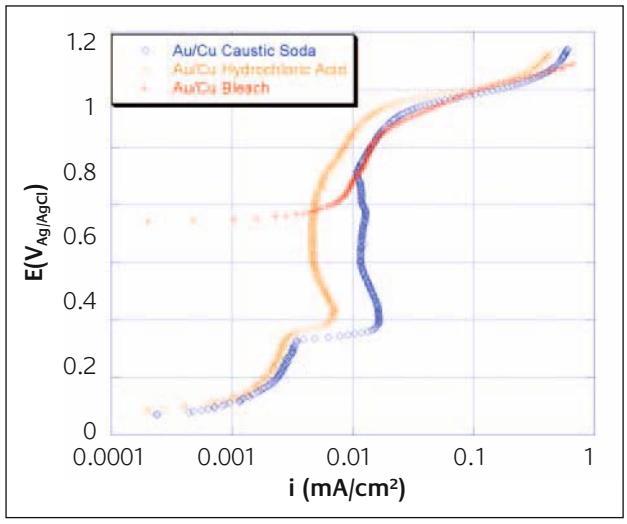

Figure 3
Polarization curves for 18K yellow gold in caustic soda, hydrochloric acid, and bleach

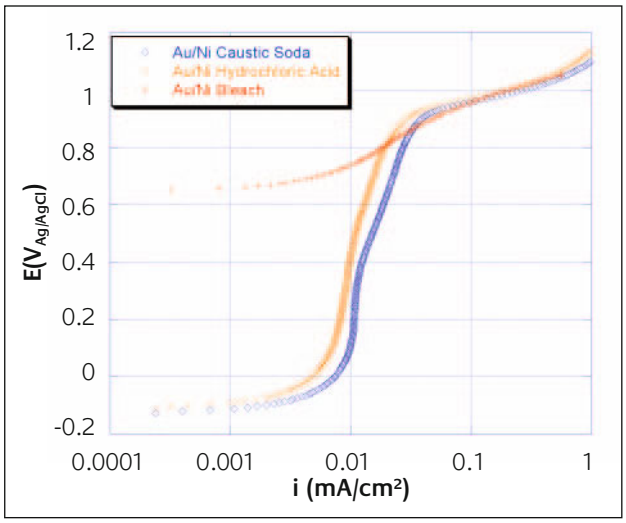

Figure 4
Polarization curves for 18K nickel white gold in caustic soda, hydrochloric acid, and bleach

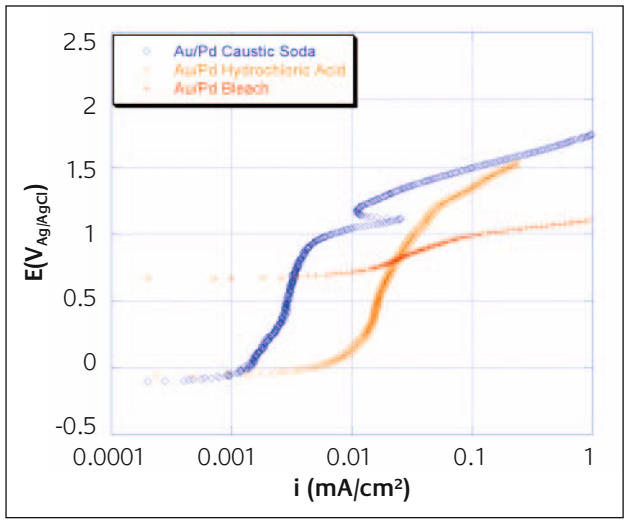

Figure 5
Polarization curves for 18K palladium white gold in caustic soda, hydrochloric acid, and bleach

increases, reaching a pseudo-passive region, where its value does not increase much beyond 0.01 mA/cm^2. At a potential of 0.9 V, defined by Pickering (14) as the critical potential (E_c), all samples show a significant increase in current density accompanied by a reddish-brown surface film formation. Once the anodic polarization test for each solution was complete, a 3% NaHS solution was dripped into the test solution to precipitate out CuS.

Figure 4 shows polarization curves for the nickel white gold alloy in the three solutions. The corrosion potentials in hydrochloric acid and caustic soda-LiquiChlor are at -0.10 V and -0.11 V, respectively. In bleach the corrosion potential was at 0.67 V. In the caustic soda and hydrochloric acid solutions there was a distinct active corrosion region prior to a pseudo-passivation at about 0.01 V. The sample tested in the bleach solution did not undergo this active-passive transition, staying strictly active. For all three solutions above the corrosion potential the current density increases, reaching a pseudo-passive region, where the value of the current density does not increase beyond about 0.01 mA/cm^2. At E_c = 0.95 V, all samples show a significant increase in current density accompanied by formation of a black surface film. Once the anodic polarization test for each solution was complete, a 3% NaHS solution was dripped into the test solution to precipitate out NiS.

Figure 5 shows polarization curves for the palladium white gold alloy in the three solutions. The corrosion potentials in the hydrochloric acid solution and caustic soda-LiquiChlor are -0.11 V and -0.12 V, respectively. In bleach the corrosion potential is at 0.7 V. In the caustic soda solution the sample shows a distinct active corrosion region prior to reaching a pseudo-passive region where the value of the current density does not increase much beyond 0.005 mA/cm^2. Passivation occurs at approximately 1.1 V followed shortly by active corrosion at 1.23 V. The sample in hydrochloric acid shows a distinct active corrosion region prior to a pseudo-passive region at approximately 0.017 mA/cm^2. At E_c = 1.25 V, the caustic soda and hydrochloric acid samples show a significant increase in current density accompanied by formation of a grayish surface film. The sample tested in the bleach solution does not undergo this active-passive transition. Once the anodic polarization test for each solution was complete, a 3% NaHS solution was dripped into the test solution. In this case no precipitate was formed indicating an absence of $PdCl_2$. The solution was then placed on a hot plate and boiled to dryness. The remnant powder was collected and shown by EDS to contain minute amounts of Pd.

Dead Weight Tests

Constant potential dead weight tests were performed in the three solutions. As shown in Table 3, the time to failure varied dramatically between alloys. The experiments showed that all three alloys suffered from IGSCC. Since all tests were done at the maximum corrosion rate, below E_c, for the system the fracture morphology was primarily intergranular (15).

Figure 6 shows an SEM image of the fracture surface of 18K

Table 3
Average Time to Failure (h)

Alloy/Solution	Hydrochloric Acid	Caustic Soda-LiquiChlor	Bleach
Au-Cu	661	573	143
Au-Ni	403	358	343
Au-Pd	DNF (1300)*	DNF (1300)*	1190

* DNF — did not fail, test discontinued after time shown in parenthesis

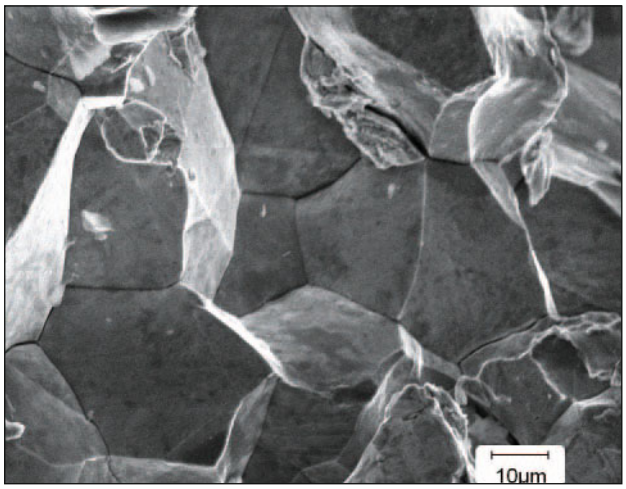

Figure 6
SEM image of the fracture surface of 18K yellow gold after dead weight testing in caustic soda-LiquiChlor. The sample fractured after 573 h at a constant potential of 128 mV

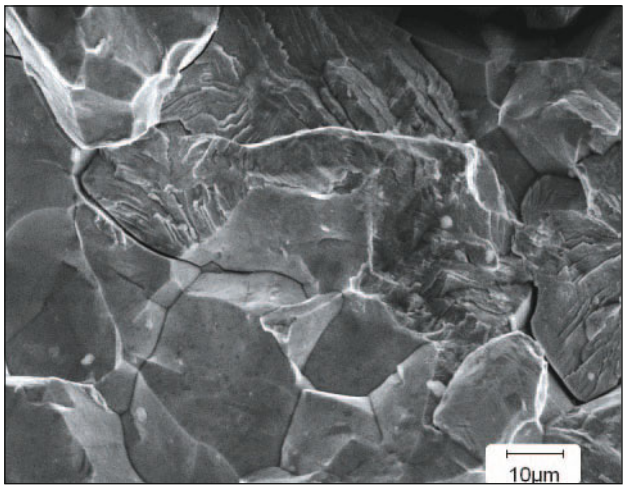

Figure 7
SEM image of the fractured surface of 18K yellow gold after dead weight testing in hydrochloric acid. The sample fractured after 661 h at a constant potential of 143 mV

yellow gold after failure in dead weight loading in caustic soda-LiquiChlor. The sample fractured in an intergranular manner after 579 h at a constant potential of 128 mV. In hydrochloric acid, the fracture was predominantly intergranular becoming transgranular as the crack reached a critical velocity and stress intensity. Figure 7 shows an example of the fracture surface, in this figure the crack moved from left to right in the image and the fracture changes from intergranular to transgranular. SEM examination of the fracture surfaces of nickel white gold samples dead weight tested in the three solutions also showed predominantly intergranular fracture with sporadic grains fracturing transgranularly as illustrated in Figure 8.

The palladium white gold samples in caustic soda-LiquiChlor and hydrochloric acid did not fracture and the tests were discontinued after 1300 h (54 days). The 18K palladium white gold samples in bleach solution fractured after 1120 h and 1190 h and, once again, showed predominantly intergranular fracture (Figure 9). The sample wires from the caustic soda and hydrochloric acid did not fail under dead weight loading, so an alternative approach was taken to verify the brittle fracture of the palladium white gold. A slow strain rate test was performed after the initial 1300 h potential-static dead weight period. A strain rate of 2.8×10^{-6} s^{-1} was used to produce fracture. The fracture surfaces of these alloys exhibit intergranular cracking eventually showing purely transgranular fracture as the crack reaches the center of the sample wire. The results obtained from all the samples are summarized in Table 4.

3 Discussion

We have demonstrated that 18K gold alloys are susceptible to failure by SCC in chlorinated solutions. The significance of these results is that they show clearly that alloys with gold concentrations in excess of 40-45 at% are not protected from SCC. Time to fracture of lower karat alloys have been shown to be as short as 1 minute (6). Whereas, for the 18K alloys used in this present study values of several hundred hours were more

Table 4
Summary of Results

Alloy	Solution	Potential for Dead weight Tests ($mV_{Ag/AgCl}$)	Fracture Mechanism	Corrosion rate (mA/cm^2)
Yellow gold	Hydrochloric acid	143	IGSCC*	1.43
Ni white gold		412	IGSCC	3.68
Pd white gold		570	DNF+	6.24
Yellow gold	Caustic soda	128	IGSCC	1.58
Ni white gold	LiquiChlor	355	IGSCC	4.26
Pd white gold		681	DNF	1.50
Yellow gold	Bleach	790	IGSCC	7.41
Ni white gold		850	IGSCC	4.37
Pd white gold		950	IGSCC	8.03

* Intergranular stress corrosion cracking
+ - Did not fail

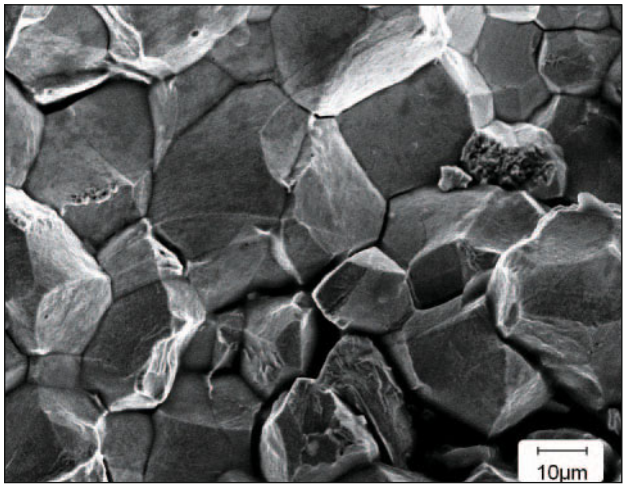

Figure 8
SEM image of the fracture surface of 18K nickel white gold after dead weight testing in bleach. Sample fractured after 343 h at a constant potential of 412 mV

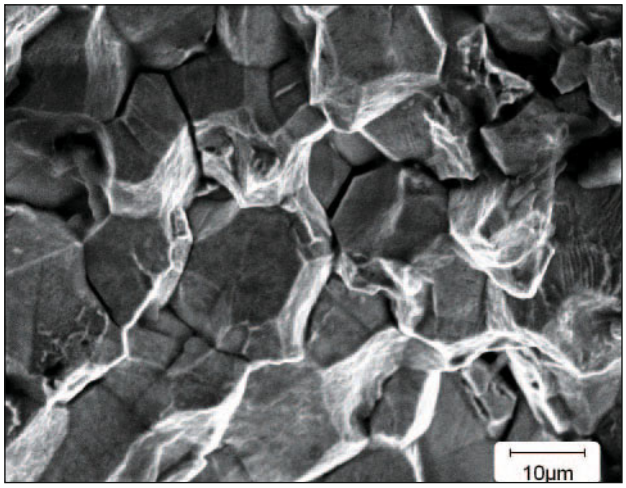

Figure 9
SEM image of fracture surface of 18K palladium white gold wire after dead weight testing in bleach. Sample fractured after 1190 h at a constant potential of 950 mV

typical, but these are still considerably shorter than expected lifetimes for gold jewelry. What is perhaps most surprising is that SCC was observed to occur in solutions with very low chlorine concentrations. In comparison, the work of Graf where failures occurred in minutes used 2% $FeCl_3$ solution (6). Based upon the half-reaction oxidation potentials, given in Table 5, of each element it is determined that the corrosion rate is controlled initially by the dissolution of Zn and the formation of $ZnCl_2$. This is followed by the dissolution of copper, nickel, or palladium below E_c (15). There is a gradual enrichment of the Cu, Ni, or Pd-depleted layer with Au producing a concomitant increase in the lattice parameter during dissolution. A time-dependent solid-solution enrichment process of the noble metal in this layer has previously been reported based on Auger spectroscopy of anodically dissolved CuAu (16) and CuPd (17) alloys below E_c. During the selective dissolution process, the Au-enriched layer is less dense than the parent material (18,19). Thus the corrosion rate based not only upon the alloying elements but also the percent Au present in the alloy.

As mentioned earlier, reported failure of in-service alloys is usually greater with yellow gold mixtures than with nickel white gold. Our observations reported in this paper lead to a different conclusion. The reason for these differences is that jewelers often electro-chemically deposit a layer of rhodium to improve the "whiteness" of nickel white gold alloys. This coating has the additional benefit of improving the corrosion resistance by placing Rh in contact with the corrosive solution instead of Ni. The oxidation potential of Ni is greater than that of Rh as shown in Table 5. The samples tested in our study did not have a surface layer of Rh.

Table 5
*Oxidation Potentials of Selected Elements**

Element	Oxidation Potential (V)
Au	-1.52
Pd	-0.92
Ag	-0.80
Rh	-0.44
Cu	-0.34
Ni	0.23
Zn	0.76

* Data from: J.A. Dean, Lange's Handbook of Chemistry 15th edition, McGraw-Hill, New York (1999) pp. 8.124-8.139

4 Conclusions

A combination of anodic polarization experiments and dead weight loading tests have demonstrated that 18K gold jewelry alloys are susceptible to SCC in a variety of common chlorinated household solutions. The polarization tests showed that the corrosion rates depended most strongly on the alloy composition and to a lesser extent on the test solution. Alloys containing zinc experienced the highest corrosion rates, due to the higher oxidation potential of zinc than the other alloy constituents. Selective dealloying was observed in the yellow gold and nickel white gold alloys but not observed in the palladium white gold alloy. As a result the palladium white gold alloys showed significant resistance to SCC in chloride containing solutions. In all cases the failure mode was predominantly intergranular fracture.

5 Acknowledgements

The authors would like to thank Pounder's Jewelry in Spokane, WA for supplying the material used in this study and Hi-Rel Laboratories for their support and guidance throughout the research.

6 About the Authors

Colin C. Merriman is a graduate student in the School of Mechanical and Materials Engineering at Washington State University. He obtained a BS in Materials Science and Engineering from Washington State University in 2005. His thesis research is focused on understanding texture development in metals.

David F. Bahr is an Associate Professor in the School of Mechanical and Materials Engineering at Washington State University. He received the Bradley Stoughton Award for Young Teachers from ASM International in 2003 and is a recipient of a Presidential Early Career Award for Scientists and Engineers. Currently he serves as the Chair of the ASM/TMS Mechanical Behavior of Materials Committee and as a Key Reader for *Metallurgical and Materials Transactions A.* He was recently appointed to the ASM International Materials Reviews Committee.

M. Grant Norton is the Herman and Brita Lindholm Endowed Chair and Professor in the School of Mechanical and Materials Engineering at Washington State University and Associate Dean of Research and Graduate Programs in the College of Engineering and Architecture. During 1999/2000 he was a visiting professor at Oxford University. He has won several awards for teaching including the ASEE Outstanding Teaching Award for the Pacific Northwest. Currently, he serves as Editor of *Journal of Materials Science.*

7 References

1 R. Herrington, C. Stanley, and R. Symes, *"Gold",* The Natural History Museum, London, 1999, p. 53

2 C.W. Corti, *Gold Bull.,* 1999, **32,** 39

3 J.D. Fritz, B.W. Parks, H.W. Pickering, *Scripta Metall* 1988, **22,** 1063

4 I.A. Maier, S.A. Fernandez, J.R. Galvele, *Corrosion Science* 1995, **37,** 1

5 B.G. Ateya, H.W. Pickering, *Corrosion Science* 1996, **38,** 1245

6 L. Graf, Stress corrosion cracking in homogeneous alloys, in *Stress Corrosion Cracking and Embrittlement,* edited by W.D. Robertson, Wiley, New York, 1956, pp. 48-60

7 J.S. Chen, M. Salmeron, T.M. Devine, *Corrosion Science* 1993, **34,** 2071

8 S.A. Serebrinsky, G.S. Duffo, and J.R. Galvele, *Corrosion Science* **1999,** 41, 191

9 W.S. Rapson and T. Groenewald, *Gold Usage,* Academic Press, London, 1978, pp. 57-64

10 G.S. Duffo, S.B. Farina, J.R. Galvele, *Corrosion Science* 2004, **46,** 1

11 G. Tammann, *Z. Anorg. Allg. Chem.* 1919, **107,** 1-240

12 M.G. Fontana, *"Corrosion Engineering",* McGraw Hill, New York, 1986, pp. 172-173

13 F.L. LaQue, N.D. Greene, *"Corrosion Basics",* NACE, Houston, TX, 1984, pp. 23-45

14 H.W. Pickering, *Corrosion Science* 1983, **23,** 1107

15 B.G. Ateya, G. Geh, A.H. Carim, H.W. Pickering, *J. Electrochem. Soc.* 2002, **149,** B27

16 J. Laurent, D. Landolt, *Electrochem. Acta* 1991, **36,** 49

17 J. Gniewek, J. Pezy, B.G. Baker, J. O'M. Bockris, *J. Electrochem. Soc* 1978, **125,** 17

18 U. Pittermann, R. Reining, K.G. Weil, *J. Electrochem. Soc* 1994, **141,** 3416

19 R. Pawlowych, D.L. Pile, H.W. Pickering, K.G. Weil, *Physical Chemistry* 1998, **207,** 113